ISSN 0915-633X

NATIONAL INSTITUTE FOR FUSION SCIENCE

Impact of Improved Confinement on Fusion Research

K. Itoh, S.-I. Itoh and A. Fukuyama

(Received – Nov. 22, 1990)

NIFS-64 Dec. 1990

RESEARCH REPORT
NIFS Series

NAGOYA, JAPAN

Impact of Improved Confinement on Fusion Research

K. Itoh*, S.-I. Itoh* and A. Fukuyama+

* National Institute for Fusion Science, Nagoya 464-01, Japan

+ Faculty of Engineering, Okayama University, Okayama 700, Japan

Abstract

The effect of the improvement of the plasma confinement (such as energy confinement time and purity and so on) on the fusion research is investigated for the ITER grade plasma. The impact of the confinement improvement is quantitatively evaluated from the view points of (1) necessary size and cost, (2) the engineering R&D (3) the economic potential and (4) reduction of the ambiguity in the design of future devices. It is shown that the confinement improvement has strong and favorable influence for these aspects.

Keywords: Improvement of confinement time,
fusion research, reactor study
cost, step size, reliability

§1 Introduction

Recent progress of the tokamak research has achieved the plasma parameter very close to the scientific demonstration of the break even condition. The deuterium-tritium plasma experiment in the near future will probably realizes the plasma with Q greater than unity (Q is the ratio of the fusion output divided by the heating power). Based on the present database, the conceptual designs of the fusion experimental reactor has been performed.[1,2] The most detailed one is the ITER activity[1].

The plasma parameter has increased by, for instance, the increments of the plasma size, current and heating power. The example of this direction of the progress is seen in three large tokamak experiments. The other kind of the progress has been achieved by exploring the elaborated controlling method and finding the improved confinement modes. The most dramatic was the discovery of the H-mode[3]. Before the finding of the H-mode, the energy confinement time of tokamaks is characterized by the degradation associated with the heating power[4,5]. This nature of the plasma, resembling to the neo-Bohm diffusion except the absolute value[6,7], would be a large obstacle in achieving the ignition in the moderate size devices. After the discovery of the H-mode, other types of the improved confinement such as Pellet mode[8], Supershot[9], Improved Ohmic Confinement (IOC)[10], Improved Divertor Confinement (IDC)[11], Improved L-mode (IL)[12] and counter injection of neutral beam[13], have been found.

The improvement of the confinement is not restricted to those in the energy confinement time. The purity of the ion species and favorable plasma profile also affect the performance of the burning plasma. In other words, merely increasing the energy confinement time is not the point, but the over-all plasma condition must be improved[14]. It must also be emphasized that the favorable character of the plasma must be maintained stationarily in the future engineering test devices. This is because the engineering test under the burning plasma would require a finite value of the fluence of the fusion output.

In advancing to the next step of the fusion research, the expectation of the plasma performance in the next step device must be reliable. This is partly because of the high price of the experimental device, but also because the engineering test can be completed only if the plasma yields the sufficient value of the fusion output. Therefore the effort to enhance the reliability of the programme will become more and more important. The improvement of the plasma confinement would enhance the safety factor in achieving the mission of the programme. The nature of the plasma under the stationary burn is not known; for instance, the asymptotic level of impurities in the time scale of hours of burning discharge is beyond present predictability. Large room of the safety factor would be necessary for the best parameter under the short discharge condition.

The objective of this article is to investigate the effect of the improvement of plasma confinement for the fusion research in proceeding to the next step. Based on the consistency analysis of the core plasma[15], we examine the influence of the confinement improvement (such as the energy confinement time, purity, plasma profile, current-drive efficiency and so on). We find that the improvements (1) reduce the system size (cost) of the experimental device with the same mission, (2) reduce the engineering R&D requirements, (3) improve economic capability and (4) make the projection more reliable. Through these effects, the improvement of plasma confinement is highly effective.

In §2, we briefly review the method of consistency analysis for the stationary burning plasma. We choose a simple relation between the plasma size and current and compare the cases with different plasma sizes. In the next section, the effect of the confinement improvement is shown. The result of the ITER activity is analysed, confirming the simple analytic modelling. By this process, the impact of the confinement improvement on the design is evaluated. Summary and discussions are given in the final section.

§2 Consistent Operation Regime

In order to evaluate the impact of the improvement of the plasma confinement, the plasma operation condition is chosen so as to satisfy the various physics constraints. The method was developed in the preceding article[15], in which the optimum performance is obtained for the given scaling laws of the plasma confinement. In this article, we also study the optimum condition by using the method of consistency analysis.

2.1 List of Physics Constraints

The necessary conditions and scaling laws are discussed in Ref.[15]. Following are the scaling laws and conditions. The major radius R and minor radius are given in [m], the plasma volume V_p is in [m^3], the magnetic field B is in [T], the electron density n_e is in [$10^{20}m^{-3}$], the temperature T is in [keV], the plasma current I_p is in [MA], and the total heating power, P, input power P_{in} and the α-particle heating power P_α are in [MW]. We assume that T_e=T_i holds, and n and T denote the volume averaged values. The line average density is given by n. κ and M denote the elongation and the ion mass number, respectively.

(1) β-limit

$$\beta < \beta_c\ (\%) = g \frac{I_p}{aB} \quad , \quad g = 2.7$$

(2) q-limit

$$q_{\psi 95\%} \geq 3$$

(3) density limit

$$\bar{n}_e < \bar{n}_c = 0.4 \frac{I_p}{a^2} (0.1P)^{\alpha} \ , \quad \alpha = 0.25$$

(4) current drive efficiency

$$I_p < \frac{CT}{nR} P_{in} \ ; \quad C = 0.026$$

(5) divertor plasma temperature

$$T_{div} < 10\mathrm{eV}, \quad T_{div}\ (\mathrm{eV}) = \frac{2.5\sqrt{P}}{n^2 \kappa a R}$$

(6) ash exhaust condition (preliminary)

$$\frac{n_e V_p}{\tau_p} > 10^4 S_{\alpha}$$

(7) energy confinement time (L-mode)

$$\tau_E^P = 0.103\ M^{0.5}\ \kappa^{0.25}\ I_p^{0.85}\ \bar{n}^{0.1}\ B^{0.3}\ a^{0.8}\ R^{0.5}\ P^{-0.5}$$

$$\tau_E^O = C_1 M^{0.5}\ \kappa a^2 + C_0 I_p^{1.4}\ B^{0.4}\ a^{-0.4}\ R^{1.4}\ P^{-1}$$

$$C_1 = 0.085, \ C_0 = 0.038$$

(8) energy confinement time (improved mode)

$$\tau_E = h\ \tau_E(\text{L-mode})$$

(9) particle confinement time

$$\tau_p = 0.05\ \bar{n}^{-1}(B/4.5)^{\delta} a\ P^{-0.5}, \quad \delta \simeq 1.5$$

The Bootstrap current is taken into account according to the formula

$$I_{BS} = \frac{10nT}{I_p}\left(\frac{a}{2}\right)^{2.5}\left(\frac{5.8}{R}\right)^{0.5} \ell^2 \tag{10}$$

when specified.

Some of the conditions (1) -(10) are reliable and some have only a small base. For instance, the distinction between two presentation for the energy confinement time is presently difficult. We use two presentations in parallel, in order to show the range of the ambiguity of the extrapolation. The estimation formula for the fusion power in terms of the plasma parameter is given in Ref.[16] and is not repeated. We assume that the temperature has the parabolic distribution, and the density profile is broader, $n(r) = n_0(1-r^2/a^2)^{0.3}$ (r is the minor radius coordinate).

2.2 Standard Parameter (L-mode)

We choose the ITER-grade parameter for the device as

$$R=5.8\ell,\ a=2\ell,\ B=4.5,\ \kappa=2,\ I_p=20\ell. \tag{11}$$

The parameter ℓ indicates the change of the size. The standard value, $\ell=1$, corresponds to $q_\psi=3$. The ratio of the deuterium and tritium is 1:1, and M is chosen to be 2.5. The introduction of the size parameter ℓ is highly idealized. In actual design, the change of the size (keeping the aspect ratio) does not cause the linear change of I_p. The model dependence Eq.(11) is assumed in order to have an analytic insight. The actual example in the design study is given in the following subsections.

Based on the L-mode scaling law, Eq.(7), the working region of steady state operation in P_{in}-n_e plane is discussed in Ref.[15]. One example is shown in Fig.1, in which the Offset-linear law is assumed for the standard parameter, $\ell=1$. The triangle ABC indicates the boundary for the consistent working region, which is determined by the β-limit, current-drive efficiency and the request for the divertor plasma temperature. The optimum value of the Q-value is 8.5. The prediction by use of the L-mode gives a large ambiguity. If one employs the power law, the maximum Q-value is given by 2.5 (at P_{in}=1GW). On the other hand, the offset-linear law predicts Q-value of 8.5 at P_{in}=0.2GW. This uncertainty, which is not resolved so long as one uses the extrapolation of the L-mode scaling law, would be a large obstacle in progressing the programme.

2.3 Dependence on the System Size

The achievable Q-value can be increased if the plasma size increases. The size dependence of the maximum Q-value for the steady state operation is given in Fig.2. The other key parameter to evaluate the economic potential is the power per unit volume

$$K = P_{fusion}/V_p. \tag{12}$$

One index for the economics is the ratio between the fusion output during the life time τ_{life} to the initial cost. If τ_{life} and the initial cost divided by V_p are approximated by constants, the K value is proportional to this ratio. In reality, K would not be a linear function of this ratio, but would be an increasing function of this ratio. The quantity K is also shown in Fig.2. In Fig.2, the power law of the L-mode scaling is employed, and the parameter ℓ is changed from 0.5 to 2.

This graph shows that the quantities Q and K can be improved by increasing the plasma size. The increment of the plasma size, however, enhances the cost of the device. The higher cost may cause the difficulty in the construction of the experimental devices and the delay of the programme. In addition to it, the increased size requires a larger R&D necessity for the engineering aspect.

To show this fact more clearly, we evaluate two quantities; one is the neutron wall loading, P_N (unit is MW/m^2), and the other is the thermal load on the divertor plate, P_{div} (unit is MW/m^2). The neutron wall loading is estimated by the ratio of the fusion neutron output to the area of the plasma surface. More exact calculations have been done in a real geometry[17]. We use a simple estimate, which is correct within a factor of 1.5, in order to have an analytic insight. The formula to estimate the divertor heat load, P_{div} is given as

$$P_{div} = C_{div} \left(\frac{P_{tot}}{V_p} \right)^{\frac{14}{11}} \left(\frac{\bar{n}_e}{n_e(a)} \right)^{\frac{7}{11}} \left(\frac{B}{\bar{n}_e q R} \right)^{\frac{7}{11}} a^{\frac{13}{11}} q R \tag{13}$$

Coefficient C_{div} and the details are discussed in the appendix. Figure 3 shows the wall loads P_N and P_{div}. It is shown that these wall loads increase when the plasma becomes bigger. The design of the heat removal is one of the key issues in designing ITER, and a substantial R&D programme is needed. If the level of P_{div} increases, the resolution of the divertor design becomes much more difficult, and much larger programme for the R&D would be required. The same argument may apply to the neutron wall loading. From these results, we see that the way of achieving the higher Q-value by larger device causes a new problems; high cost and longer time scale for the next step, and the increased requests for the engineering R&D.

§3 Effect of the Improved Confinement

3.1 Confinement Improvement and Evaluation

There is an alternative approach to enhance the expected Q-value for the next step devices. The plasma confinement can be improved (or deteriorated) in the following aspects:

(a) energy confinement time

(b) purity of the fuel ions

(c) plasma profile

(d) β-limit

(e) current-drive efficiency

and so on. The main part of the present tokamak research is to make progress in these aspects of the plasma.

The improved confinement mode has been found and studied intensively. Other points, (b)-(e), also have a lot of database. In this article, we assume that the progresses in directions (a) to (e) can be gained <u>independently</u>, and study the impact of the improvements. In actual plasmas, these improvements are not realized independently. It has been, for instance, well known that the improved modes are often associated with the increased impurity level. The optimization of the β-limit requires particular profiles, which may not be consistent with the increased fusion rate. The analysis here is done to find the effects of these improvements and the critical path to reach the better confinement state. The trade-off can be solved if the sensitivity to each elements are analysed.

We evaluate the following quantities;

(i) Q-value and K-value

(ii) Necessary size to reach the Q-value of mission

(iii) Wall loadings P_{div} and P_N.

As is discussed in the previous section, quantities in (i) are related to the economic potential, those in (ii) to the cost and time scale of the research, and those in (iii) to the necessary level of the engineering R&D.

3.2 Effect of Improvement of τ_E

We study the influence of the improvement in the energy confinement time. As is discussed in §3.1, we change the parameter h (ratio of τ_E to the L-mode scaling law) independently from other parameters such as the fuel purity.

Figure 4 illustrates the Q-value and K-value for the fixed plasma size (ℓ=1). It is shown that the power amplification factor Q increases strongly while the K-value (power density) reduces slowly. The reduction of the power density is due to the increment of the ion temperature. (If the temperature becomes too high, the fusion cross section of D/T-reaction has weaker dependence than T^2 and the power density starts to degrade. In this case, the other reaction process, D/D or D/^{3}He, has contributions.)

The improvement of the confinement time, contrary to the case of increasing the size, can also reduce the engineering R&D requests. Figure 5 illustrates the wall loadings P_N and P_{div} as a function of the parameter h (ℓ is fixed to be unity.) As the enhancement parameter h increases, the wall loading reduces. The reduction is prominent for the heat load onto the divertor plate, while the neutron loading does not change much. The condition on the divertor plate becomes relaxed. This would be very helpful in designing the ITER grade devices.

We finally study the necessary size of the plasma to obtain the high Q-value as a function of the improvement factor. Figure 6 shows the contour of the Q-value on the h-ℓ plane. The solid line is for the case of the power law and the dashed lines for the offset-linear law. In order to achieve the necessary Q-value under the steady state operation, the size obeys the relation

$$\ell \sim \begin{cases} 1.9\ h^{-1.3}\ (Q=10) \\ 1.4\ h^{-1.4}\ (Q=5) \end{cases} \quad \text{(power law)} \qquad (14\text{-}1)$$

$$\ell \sim \begin{cases} 1.0\ h^{-0.6}\ (Q=10) \\ 0.8\ H^{-0.6}\ (Q=5) \end{cases} \quad \text{(offset-linear law)} \qquad (14\text{-}2)$$

These results clearly show the reduction of the necessary plasma size and associated cost of the device. The period for the construction also reduces due to the smaller size.

It is also noted that the ambiguity in the prediction can also be reduced by the improved confinement time. The figure 6 shows the difference of the necessary size between the predictions of the power law and offset-linear law. The former scaling law predicts that the linear scale of $\ell=1.4$ is necessary while the latter gives the value of $\ell=0.8$ in order to obtain Q=5. On the other hand, if the enhancement factor of 2 is possible, then the necessary size reduces to about $\ell=0.6$ (Q=5) and $\ell=0.8$ (Q=10), and that the necessary size weakly depends on the choice of the scaling law. The ambiguity in the extrapolation is reduced, which is inevitable in advancing the program to the next step.

Summarizing the above results, we show how the requests for the engineering R&D and economic potential change in Figs.7 and 8. The figure 7 illustrates the change of (P_{div}, P_N) according to that of (h, ℓ). Figure 8 shows that for (Q, K).

One of the characteristics of the (P_{div}, P_N) diagram is that the region of the parameter is limited to a narrow regime even though h and ℓ changes by the factor of 2. It is also noted that, when the improvement is not realized (i.e., $h \sim 1$), the change in the size greatly increases the level of the wall loading. On the other hand, if the sufficient improvement is realized (such as $h \sim 2$), the increment of the size does not require the increment of the wall loading. The increase of the size can improve the economic potential, as is shown in Fig.8. We conclude that the optimum condition from the view point of the economic potential can be looked for without increasing the request for the engineering R&D.

The axis of P_{div} in figures are given in the arbitrary unit. One example of the estimation of the absolute value is shown. Reference [18] numerically estimates the peak heat load using a two-dimensional simulation code. According to the discussion in the appendix, the value of P_1 in Fig.7 corresponds to $10MW/m^2$. If the heat loads to the inside divertor trace and outside trace are balanced, then the value of P_2 in Fig.7 corresponds to $10MW/m^2$. Thus the control in the heat flux in the scrape-off layer can also reduce the engineering R&D task.

3.3 Example from the Design Study

The relation (11) in changing the size is for the analytic study and too idealized. Hence the relation (14) may not be taken too seriously. The analysis of the impact on the system size and cost needs at least a conceptual design. We study the design activity for the ITER.

The conceptual design of the ITER has been performed by introducing the enhancement factor h. The change of the size and cost owing to the change of the enhancement factor are graphically presented in reports. In the ITER report[17], following parameters are fixed; $B_T(max)=11T$, $B_{OHcoil}(max)=12T$,

$\kappa=2$, $q_{cyl}=0.844$, and $Z_{eff}=1.78$. In addition to it, the sum of the toroidal coil thickness and the half of the OH coil, d_c, and the distance of the plasma inner surface from the toroidal coil surface, d_B, are kept constant, simulating the real coil systems. The constraints are chosen that T=10keV and operation point is fixed to the β-limit. By using these assumptions, the necessary value of h for the ignition condition (i.e., the condition for the full current-derive is not requested in this case) is obtained.

From this analysis (with R/a=3), one can see the relations between the necessary size, current and improvement factor. In the parameter regime of interest, I_p follows the relation $I_p \propto \ell^{1.5}$, not ℓ^1. If one chooses the offset-linear law (Shimomura-Odajima law[19]), the results are fitted to the estimations

$$I_p \propto h^{-0.8}, \tag{15}$$

$$\$ \propto h^{-1.3} \tag{16}$$

where \$ is the relative cost of the device.

The reduction of the plasma size which comes from the enhancement factor h is annihilated if the impurity increases. Taking the parameters h and Z_{eff}, the contours of the necessary current is given in Ref.[17].

§4 Summary and Discussion

In this article, we study the impact of the improvement of the plasma confinement in the fusion research. Based on the study of the ITER grade plasma, we find that the improvement of the confinement (such as τ_E, purity of the fuel, plasma profile, and so on)

(a) can reduce the necessary size and cost of the experimental reactor,

(b) can reduce the wall loading and hence the necessary engineering R&D task,

(c) can increase the economic potential, and

(d) can reduce the ambiguity in the projection for the next step device.

These effects make it easier to progress to the next step and the mission more plausible. According to the design activity of ITER, the necessary cost of the device is proportional to approximately $h^{-1.3}$ (in case of Shimomura-Odajima scaling). The alternate approach to increase the Q-value, i.e., making the plasma larger, is also studied. In this case, however, the requirement for the engineering R&D becomes large in addition to the increased cost for the construction.

It should be noted that the impact is favourable, if the over all improvement is realized. It has been known that the Q-value may be approximately proportional to

$$H = h\ \tau_p\ (1-f_d)^2,$$

when the achievable Q-value is limited by the input power. In this representation, τ_p is the peakedness of the plasma pressure, $n(0)T(0)/nT$, and f_d is the level of dilution of the fuel, $f_d = \Sigma Z_I n_I/n_e$, where the summation is taken over impurities. If Q can be large, the H is defined by $h\tau(1-f_d)$. Even though the enhancement factor h is large, the impact is small if the overall parameter H is low due to, for instance, the accumulation of impurities. The overall evaluation on the presently-observed improved modes has been performed and given in Ref.[14].

We finally note on the possibility of the advanced fusion reaction. Fusion reaction based on such as D/D or D/^{3}He has advantage from the view point of the radio activation of the system. These reaction can be realized if and only if the confinement time is long enough. The present analysis only studies the effect of the improved confinement for the near future research, i.e., the range of $h \sim 2$. If the range of improvement is extended, the reaction based on the advanced fusion would be possible. Such impact would be more profound and requires further study.

Acknowledgements

Part of the paper is prepared for the database of the Panel of the Japan Atomic Energy Commission. Authors acknowledge discussions of the other members of the Panel, Drs. M. Fujiwara, H. Maeda, S. Matsuda, H. Obayashi, Y. Shimomura, H. Toyama, T. Tsunematsu, K. Yamamoto, and M. Wakatani. Discussions with Drs. T. Mizoguchi, T. Takizuka and N. Ueda, are also appreciated. This work is partly supported by the Grant-in-Aid for Scientific Research of MoE, the collaboration programme between JAERI and universities on fusion research, and the Japan Society of Plasma Physics and Nuclear Fusion.

Appendix: Divertor Heat Load

Divertor functioning is characterized by such as

(a) Divertor heat load, P_{div}

(b) Impurity back flow to the core plasma

(c) Pumping efficiency

(d) Erosion rate of the plate

(e) Radiation and charge exchange from divertor plasma.

One of the key parameters is the plasma temperature in front of the divertor plate (or in front of the sheath). Plasma temperature T_{div} is used as one of the physics constraints. We here estimate the divertor heat load based on the analytic calculation and numerical simulation.

The peak heat load does not directly constrain the core plasma parameter. This parameter is strongly related to the plausibility of the long pulse operation. The peak heat load is determined by two quantities, the total power and the width of the heat channel on the plate. We evaluate the scaling of the peak heat load.

The flow of the energy in the scrape-off layer (SOL) is determined by the competition between the flow along the field line and the cross-field diffusion. The heat load onto the divertor plate is given by

$$P_{div} = \frac{\eta P_{out}}{2\pi R\Delta} \quad \text{(A1)}$$

where P_{out} is the power flow to the SOL region from the core, η is the rate of the heat flow onto the divertor plate (ratio of $1-\eta$ corresponds to the remote radiative cooling in the SOL region), and Δ is the heat channel width. We evaluate P_{out} by $P_{in}+P_{\alpha}$.

The scaling of Δ is derived in literatures[20,21]. We assume that the parallel heat conduction is classical. The cross field heat diffusivity is given by the heat conductivity κ , which is given as

$$\kappa_{\perp} = \alpha\left(\frac{nT_e}{16eB}\right) \tag{A2}$$

(α is a numerical coefficient). If the coefficient α is constant, then we have the scaling law

$$\frac{\Delta}{a} \propto \left(\frac{\eta P_{tot}}{aR}\right)^{-\frac{3}{11}} a^{-\frac{3}{11}} \left(\frac{n_b}{R}\right)^{\frac{7}{11}} \left(\frac{B_T}{B_p}\right)^{\frac{4}{11}} \tag{A3}$$

It is noted that the width Δ does not necessarily scale as ℓ^1, but depends on other plasma parameters. By using this results, we have

$$P_{div} = C_{div} \cdot \left(\frac{\eta P_{tot}}{V_p}\right)^{\frac{14}{11}} \left(\frac{\overline{n}_e}{n_e(a)}\right)^{\frac{7}{11}} \left(\frac{B}{\overline{n}_e qR}\right)^{\frac{7}{11}} qRa^{\frac{13}{11}} \tag{A4}$$

The peak heat load depends on the power density, P/V_p, peakedness of the density, $\overline{n}/n(a)$, density and size. The coefficient C_{div} depends on the actual shape of the divertor chamber, divertor plate material, pumping speed and the working gas.

The scaling law (A4) depends on the choice of the model of the cross field diffusion coefficient and may contain the ambiguity. Because the true form of the transport coefficient in the SOL region has not been obtained, we here take other form of the diffusivity and study the range of the error in the prediction. In the core plasma, the ratio of the diffusivity to the Bohm diffusion depends on the gyroradius. If one assumes that the coefficient α depends on the plasma parameter such as

$$\alpha \propto \rho/a, \tag{A5}$$

then the peak heat load scales as

$$\hat{P}_{div} \propto \left(\frac{P_{tot}}{\ell^3}\right)^{\frac{7}{6}} \ell^{\frac{23}{12}} \left(\frac{n(a)}{B^2}\right)^{-\frac{7}{12}} \tag{A6}$$

Figure A1 illustrates the ℓ dependence of P_{div} (solid line)and $\hat{P}_{div}$ (dashed line) for the case of the power law and offset-linear law.

The coefficient C_{div} is determined by the numerical simulation. Reference [18] gives the simulation result, and the peak heat load P_{div} reaches $7.5 MW/m^2$ for the parameter of P_{out} = 240MW, edge density of $n_e(a)=4 \times 10^{19} m^{-3}$, and the double null configuration. The in-out asymmetry of the heat flux is assumed, and 80% is deposited onto the outside. If this asymmetry is resolved, then the peak heat load would reduce to $4.1 MW/m^2$.

References

[1] ITER Concept Definition (IAEA, Vienna, 1989) Vol.1 and 2 (ITER Documentation Series 2 and 3).

[2] FER Team, "Conceptual Design of the Fusion Engineering Device" (JAERI, 1990) to be presented in 13th International Conference on Plasma Physics and Controlled Nuclear Fusion Research.

[3] F. Wagner, et al., Phys. Rev. Lett. 49 (1982) 1408.

[4] R. Goldston, Plasma Phys. Controlled Fusion 26 (1984) 87.

[5] S. M. Kaye, Phys. Fluids 28 (1985) 2327.

[6] T. Ohkawa, et al., in 2nd International Conference on Plasma Physics and Controlled Nuclear Fusion Research (IAEA, Culham, 1965), Nucl. Fusion Suppl. (1966, IAEA, Vienna) Vol.1 p103, 145.

[7] S. Yoshikawa, Nucl. Fusion 13 (1973) 433.

[8] M. Greenwald, et al., Phys. Rev. Lett. 53 (1984) 352.

[9] R. J. Hawryluk, et al., in 11th International Conference on Plasma Physics and Controlled Nuclear Fusion Research (IAEA, Kyoto, 1986), Nucl. Fusion Suppl. (1987, IAEA, Vienna) Vol.1 p51.

[10] F.X. Soldner, et al., Phys. Rev. Lett. 61 (1988) 1105.

[11] S. Tsuji and JT-60 Team, in 12th International Conference on Plasma Physics and Controlled Nuclear Fusion Research (IAEA, Nice, 1988), Nucl. Fusion Suppl. (1989, IAEA, Vienna) Vol.1

[12] M. Mori, et al., Nucl. Fusion 28 (1988) 1892.

[13] G. Fussmann, et al., in 12th International Conference on Plasma Physics and Controlled Nuclear Fusion Research (IAEA, Nice, 1988), Nucl. Fusion Suppl. (1989, IAEA, Vienna) Vol.

[14] S.-I. Itoh, H. Maeda and Y. Miura, "Evaluation of the confinement improvement for various improved confinement mode" to be published in Kakuyugo Kenkyu (1990).

[15] S.-I. Itoh, A. Fukuyama, T. Takizuka and K. Itoh, Fusion Technology 16 (1989) 346.

[16]T. Takizuka and M. Yamagiwa, "Reactivity of DT plasma with beam-induced tail in magnetic confinement system", JAERI-M 87-066 (1987).
[17] W. Spears, T. Mizoguchi, J. Perkins, S. Putvinskij, C. Flanagan, "Design Point Selection for an Ignited ITER" (ITER Documentation Series 5, 1989).
[18] N. Ueda and M. Tanaka, "Computer Modelling of Boundary Plasmas in Tokamaks" Nuclear Engineering (1990) in press.
[19] Y. Shimomura and K. Odajima, Comments Plasma Phys. Controlled Fusion 10 (1987) 207.
[20] F. Wagner and K. Lackner, in Physics of the Plasma Wall Interactions in Controlled Fusion (ed. D.E. Post and H. Behrisch, NATO ASI Series B131, Plenum Press, 1984) 931.
[21] S.-I. Itoh, N. Ueda, and K. Itoh, "Simulation study of scalings in scrape-off layer plasma by two-dimensional transport code", Plasma Phys. Controlled Fusion 32 (1990) in press.

Figure Captions

Fig. 1 Operation diagram on the n_e-P_{in} plane. Standard size (ℓ=1, I_p=20MA), and the Offset linear law of L-mode is chosen. Criteria for the density limit, divertor plasma temperature, current drive, beta limit, and ash exhaust are shown. The region ABC is the consistent working region for the steady state operation. Contours of the Q-value and temperature are also shown. The maximum Q-value is realized at the point C, where Q is approximately 8.5 and input power is 215MW. The bootstrap current is not taken into account.

Fig. 2 The size dependence of the Q-value and the power density K. L-mode scaling (power law) is chosen.

Fig. 3 Dependence of the wall loading on the size parameter ℓ. The power law for the L-mode is chosen.

Fig. 4 The dependence of the Q-value and the power density K-value on the enhancement factor h. Plasma size is standard (ℓ=1) and the power law is chosen.

Fig. 5 Dependence of the wall loading on the enhancement factor h.

Fig. 6 Contour of Q-values on the h-ℓ plane. Solid lines are for the case of the offset-linear law, and dashed lines for the power law. Steady state operation condition with Z_{eff}=1 are assumed.

Fig. 7 The response of the wall loadings to the change of (h, ℓ). The range of (h, ℓ) and corresponding points (ABCD) are given in (b).

Fig. 8 The response of the parameter (P/V_p, Q) to the change of (h, ℓ). Points (ABCD) are given in Fig. 7(b). The results of O-law and P-law are compared.

Fig. A1 The peak heat load at the divertor plate as a function of the plasma size. Steady state condition with L-mode scaling is used. Solid lines shows P_{div}, and dashed lines show $\hat{P}_{div}$. P and O indicate the power law and offset-linear law. Values are normalized at ℓ=1.

Fig. 1

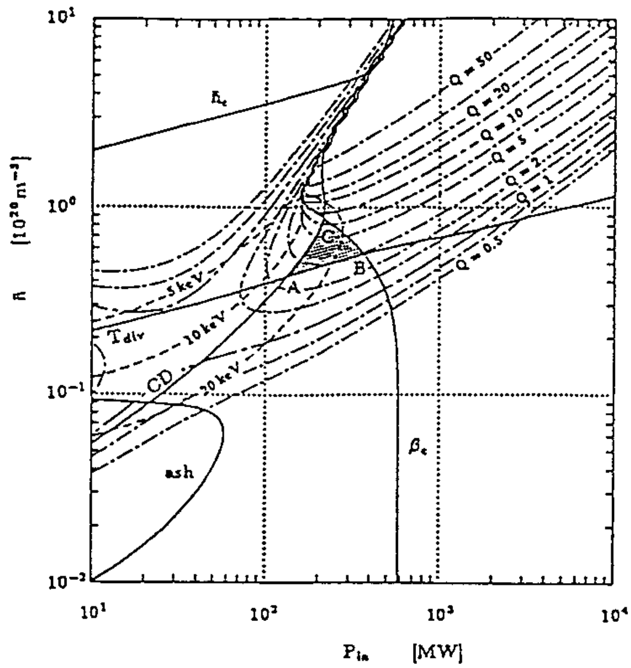
$\bar{n}$ $[10^{20}\,m^{-3}]$
P_{in} [MW]
$\bar{n}_c$
β_c
ash
T_{div}
CD
5 keV
10 keV
20 keV
A
B
C
Q = 50
Q = 20
Q = 10
Q = 5
Q = 2
Q = 1
Q = 0.5

Fig. 2

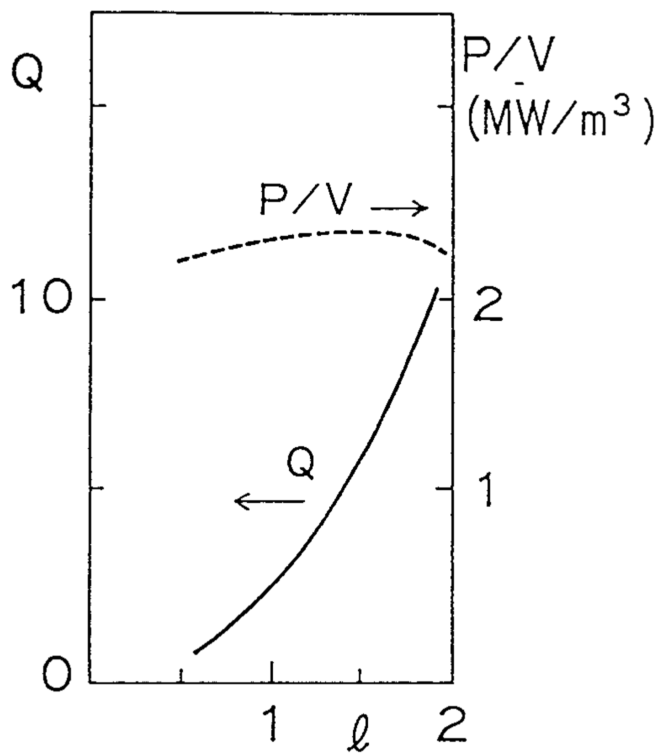

Fig. 3

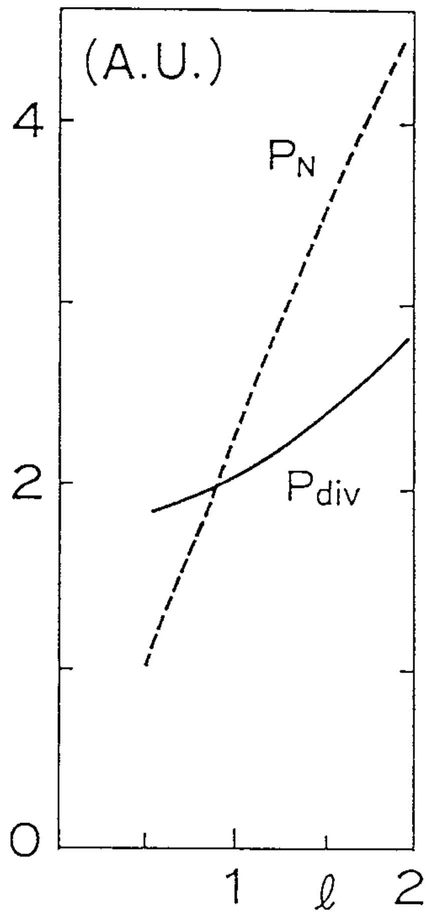

Fig.4

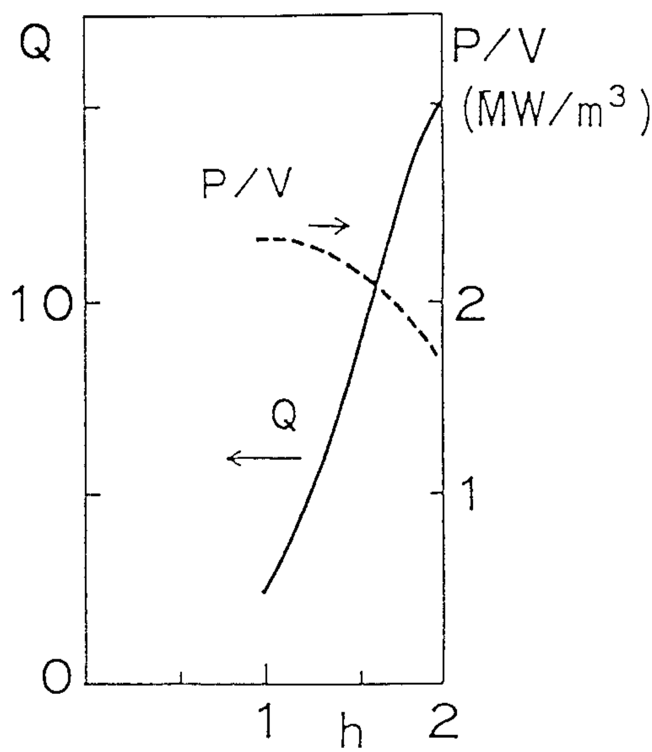

Fig.5

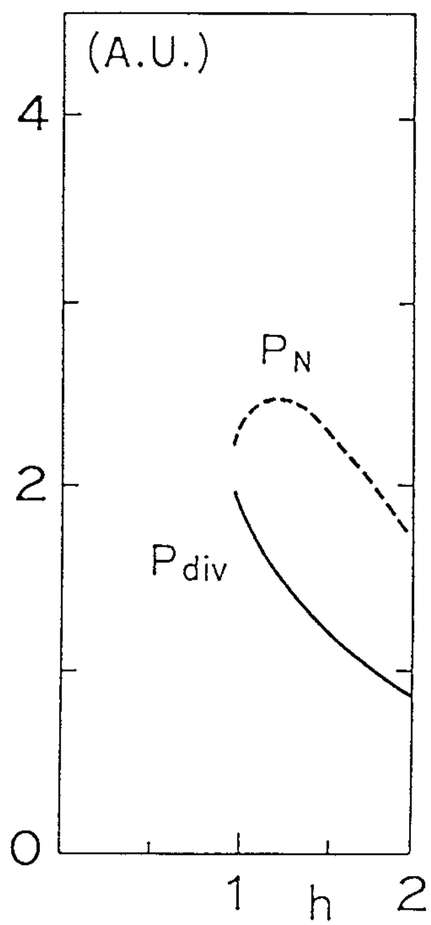

Fig. 6

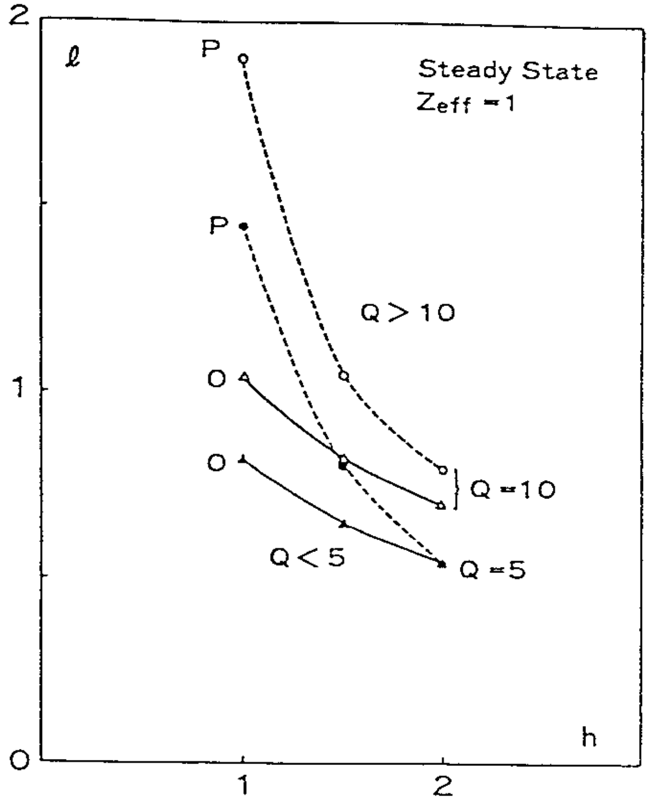

Fig7.(a)

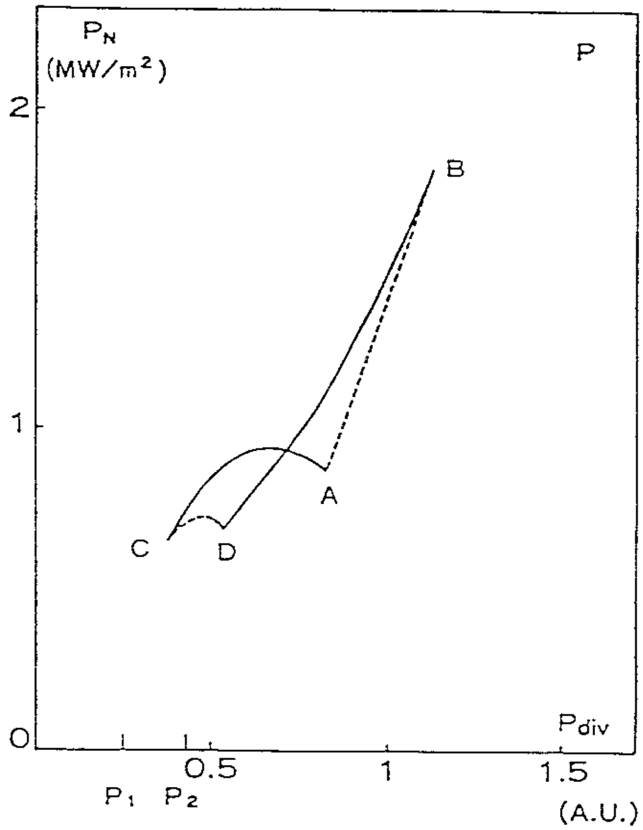

Fig.7(b)

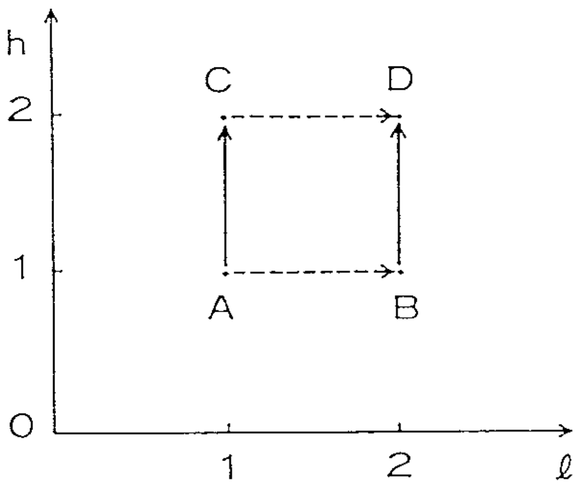

Fig. 8

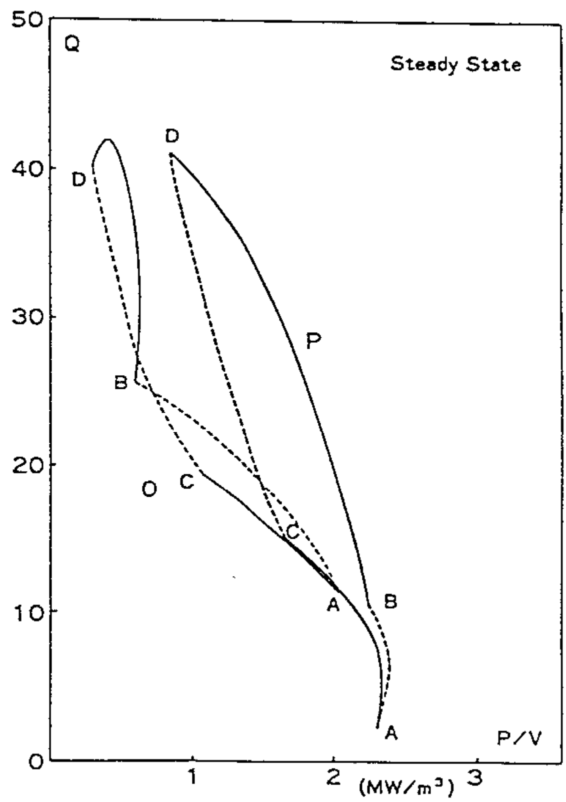

Fig. A1

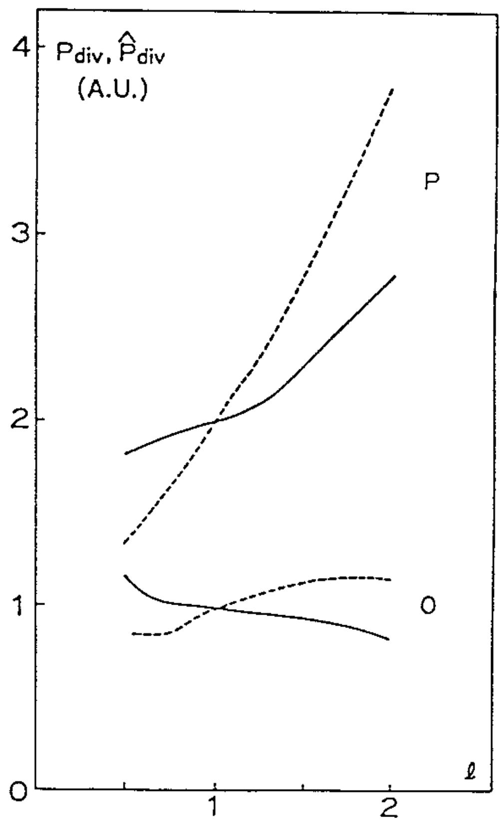

Recent Issues of NIFS Series

NIFS-34 K. Hamamatsu, A. Fukuyama, S.-I. Itoh, K. Itoh and M. Azumi, *RF Helicity Injection and Current Drive* ; July 1990

NIFS-35 M. Sasao, H. Yamaoka, M. Wada and J. Fujita, *Direct Extraction of a Na- Beam from a Sodium Plasma* ; July 1990

NIFS-36 N. Ueda, S.-I. Itoh, M. Tanaka and K. Itoh, *A Design Method of Divertor in Tokamak Reactors* Aug. 1990

NIFS-37 J. Todoroki, *Theory of Longitudinal Adiabatic Invariant in the Helical Torus*; Aug. 1990

NIFS-38 S.-I. Itoh and K. Itoh, *Modelling of Improved Confinements – Peaked Profile Modes and H-Mode–* ; Sep. 1990

NIFS-39 O. Kaneko, S. Kubo, K. Nishimura, T. Syoji, M. Hosokawa, K. Ida, H. Idei, H. Iguchi, K. Matsuoka, S. Morita, N. Noda, S. Okamura, T. Ozaki, A. Sagara, H. Sanuki, C. Takahashi, Y. Takeiri, Y. Takita, K. Tsuzuki, H. Yamada, T. Amano, A. Ando, M. Fujiwara, K. Hanatani, A. Karita, T. Kohmoto, A. Komori, K. Masai, T. Morisaki, O. Motojima, N. Nakajima, Y. Oka, M. Okamoto, S. Sobhanian and J. Todoroki, *Confinement Characteristics of High Power Heated Plasma in CHS*; Sep. 1990

NIFS-40 K. Toi, Y. Hamada, K. Kawahata, T. Watari, A. Ando, K. Ida, S. Morita, R. Kumazawa, Y. Oka, K. Masai, M. Sakamoto, K. Adati, R. Akiyama, S. Hidekuma, S. Hirokura, O. Kaneko, A. Karita, T. Kawamoto, Y. Kawasumi, M. Kojima, T. Kuroda, K. Narihara, Y. Ogawa, K. Ohkubo, S. Okajima, T. Ozaki, M. Sasao, K. Sato, K.N. Sato, T. Seki, F. Shimpo, H. Takahashi, S. Tanahashi, Y. Taniguchi and T. Tsuzuki, *Study of Limiter H- and IOC- Modes by Control of Edge Magnetic Shear and Gas Puffing in the JIPP T-IIU Tokamak*; Sep. 1990

NIFS-41 K. Ida, K. Itoh, S.-I. Itoh, S. Hidekuma and JIPP T-IIU & CHS Group, *Comparison of Toroidal/Poloidal Rotation in CHS Heliotron/Torsatron and JIPP T-IIU Tokamak*; Sep .1990

NIFS-42 T.Watari, R.Kumazawa,T.Seki, A.Ando,Y.Oka, O.Kaneko, K.Adati, R.Ando, T.Aoki, R.Akiyama, Y.Hamada, S.Hidekuma, S.Hirokura, E.Kako, A.Karita, K.Kawahata, T.Kawamoto, Y.Kawasumi, S.Kitagawa, Y.Kitoh, M.Kojima, T. Kuroda, K.Masai, S.Morita, K.Narihara, Y.Ogawa, K.Ohkubo, S.Okajima, T.Ozaki, M.Sakamoto, M.Sasao, K.Sato, K.N.Sato, F.Shinbo, H.Takahashi, S.Tanahashi, Y.Taniguchi, K.Toi, T.Tsuzuki, Y.Takase, K.Yoshioka, S.Kinoshita, M.Abe, H.Fukumoto, K.Takeuchi, T.Okazaki and M.Ohtuka, *,Application of Intermediate Frequency Range Fast Wave to JIPP T-IIU and HT-2 Plasma*; Sep. 1990

NIFS-43 K.Yamazaki, N.Ohyabu, M.Okamoto, T.Amano, J.Todoroki, Y.Ogawa, N.Nakajima, H.Akao, M.Asao, J.Fujita, Y.Hamada, T.Hayashi, T.Kamimura, H.Kaneko, T.Kuroda, S.Morimoto, N.Noda, T.Obiki, H.Sanuki, T.Sato, T.Satow, M.Wakatani, T.Watanabe, J.Yamamoto, O.Motojima, M.Fujiwara, A.Iiyoshi and LHD Design Group, *Physics Studies on Helical Confinement Configurations with l=2 Continuous Coil Systems*; Sep. 1990

NIFS-44 T.Hayashi, A.Takei, N.Ohyabu, T.Sato, M.Wakatani, H.Sugama, M.Yagi, K.Watanabe, B.G.Hong and W.Horton, *Equilibrium Beta Limit and Anomalous Transport Studies of Helical Systems*; Sep. 1990

NIFS-45 R.Horiuchi, T.Sato, and M.Tanaka, *Three-Dimensional Particle Simulation Study on Stabilization of the FRC Tilting Instability*; Sep. 1990

NIFS-46 K.Kusano, T.Tamano and T. Sato, *Simulation Study of Nonlinear Dynamics in Reversed-Field Pinch Configuration*; Sep. 1990

NIFS-47 Yoshi H.Ichikawa, *Solitons and Chaos in Plasma*; Sep. 1990

NIFS-48 T.Seki, R.Kumazawa, Y.Takase, A.Fukuyama, T.Watari, A.Ando, Y.Oka, O.Kaneko, K.Adati, R.Akiyama, R.Ando, T.Aoki, Y.Hamada, S.Hidekuma, S.Hirokura, K.Ida, K.Itoh, S.-I.Itoh, E.Kako, A. Karita, K.Kawahata, T.Kawamoto, Y.Kawasumi, S.Kitagawa, Y.Kitoh, M.Kojima, T.Kuroda, K.Masai, S.Morita, K.Narihara, Y.Ogawa, K.Ohkubo, S.Okajima, T.Ozaki, M.Sakamoto, M.Sasao, K.Sato, K.N.Sato, F.Shinbo, H.Takahashi, S.Tanahashi, Y.Taniguchi, K.Toi and T.Tsuzuki, *Application of Intermediate Frequency Range Fast Wave to JIPP T-IIU Plasma*; Sep.1990

NIFS-49 A.Kageyama, K.Watanabe and T.Sato, *Global Simulation of the Magnetosphere with a Long Tail: The Formation and Ejection of Plasmoids*; Sep.1990

NIFS-50 S.Koide, *3-Dimensional Simulation of Dynamo Effect of Reversed Field Pinch*; Sep. 1990

NIFS-51 O.Motojima, K. Akaishi, M.Asao, K.Fujii, J.Fujita, T.Hino, Y.Hamada, H.Kaneko, S.Kitagawa, Y.Kubota, T.Kuroda, T.Mito, S.Morimoto, N.Noda, Y.Ogawa, I.Ohtake, N.Ohyabu, A.Sagara, T. Satow, K.Takahata, M.Takeo, S.Tanahashi, T.Tsuzuki, S.Yamada, J.Yamamoto, K.Yamazaki, N.Yanagi, H.Yonezu, M.Fujiwara, A.Iiyoshi and LHD Design Group, *Engineering Design Study of Superconducting Large Helical Device*; Sep. 1990

NIFS-52 T.Sato, R.Horiuchi, K. Watanabe, T. Hayashi and K.Kusano, *Self-Organizing Magnetohydrodynamic Plasma*; Sep. 1990

NIFS-53 M.Okamoto and N.Nakajima, *Bootstrap Currents in Stellarators and Tokamaks*; Sep. 1990

NIFS-54 K.Itoh and S.-I.Itoh, *Peaked-Density Profile Mode and Improved Confinement in Helical Systems*; Oct. 1990

NIFS-55 Y.Ueda, T.Enomoto and H.B.Stewart, *Chaotic Transients and Fractal Structures Governing Coupled Swing Dynamics*; Oct. 1990

NIFS-56 H.B.Stewart and Y.Ueda, *Catastrophes with Indeterminate Outcome*; Oct. 1990

NIFS-57 S.-I.Itoh, H.Maeda and Y.Miura, *Improved Modes and the Evaluation of Confinement Improvement*; Oct. 1990

NIFS-58 H.Maeda and S.-I.Itoh, *The Significance of Medium- or Small-size Devices in Fusion Research*; Oct. 1990

NIFS-59 A.Fukuyama, S.-I.Itoh, K.Itoh, K.Hamamatsu, V.S.Chan, S.C.Chiu, R.L.Miller and T.Ohkawa, *Nonresonant Current Drive by RF Helicity Injection*; Oct. 1990

NIFS-60 K.Ida, H.Yamada, H.Iguchi, S.Hidekuma, H.Sanuki, K.Yamazaki and CHS Group, *Electric Field Profile of CHS Heliotron/Torsatron Plasma with Tangential Neutral Beam Injection*; Oct. 1990

NIFS-61 T.Yabe and H.Hoshino, *Two- and Three-Dimensional Behavior of Rayleigh-Taylor and Kelvin-Helmholz Instabilities*; Oct. 1990

NIFS-62 H.B. Stewart, *Application of Fixed Point Theory to Chaotic Attractors of Forced Oscillators;* Nov. 1990

NIFS-63 K.Konno, M.Mituhashi and Yoshi H.Ichikawa, *Soliton on Thin Vortex Filament;* Dec. 1990

NIFS DATA-1 Y. Yamamura, T. Takiguchi and H. Tawara, *Data Compilation of Angular Distributions of Sputtered Atoms* ; Jan. 1990

NIFS DATA-2 T. Kato, J. Lang and K. E. Berrington, *Intensity Ratios of Emission Lines from OV Ions for Temperature and Density Diagnostics* ; Mar. 1990

NIFS DATA-3 T. Kaneko, *Partial Electronic Straggling Cross Sections of Atoms for Protons* ; Mar. 1990

NIFS DATA-4 T. Fujimoto, K. Sawada and K. Takahata, *Cross Section for Production of Excited Hydrogen Atoms Following Dissociative Excitation of Molecular Hydrogen by Electron Impact* ; Mar. 1990

NIFS DATA-5 H. Tawara, *Some Electron Detachment Data for H- Ions in Collisions with Electrons, Ions, Atoms and Molecules – an Alternative Approach to High Energy Neutral Beam Production for Plasma Heating–* ; Apr. 1990

NIFS DATA-6 H. Tawara, Y. Itikawa, H. Nishimura, H. Tanaka and Y. Nakamura, *Collision Data Involving Hydro-Carbon Molecules* ; July 1990

NIFS DATA-7 H.Tawara, *Bibliography on Electron Transfer Processes in Ion-Ion/Atom/Molecule Collisions –Updated 1990–*; Oct. 1990

NIFS TECH-1 H. Bolt and A. Miyahara, *Runaway–Electron –Materials Interaction Studies* ; Mar. 1990

NIFS PROC-1 *U.S.-Japan Workshop on Comparison of Theoretical and Experimental Transport in Toroidal Systems Oct. 23-27, 1989* ; Mar. 1990

NIFS PROC-2 *Structures in Confined Plasmas –Proceedings of Workshop of US-Japan Joint Institute for Fusion Theory Program–* ; Mar. 1990

NIFS PROC-3 *Proceedings of the First International Toki Conference on Plasma Physics and Controlled Nuclear Fusion –Next Generation Experiments in Helical Systems– Dec. 4-7, 1989* ; Mar. 1990

NIFS PROC-4 *Plasma Spectroscopy and Atomic Processes –Proceedings of the Workshop at Data & Planning Center in NIFS–*; Sep. 1990

NIFS PROC-5 *Symposium on Development of Intensed Pulsed Particle Beams and Its Applications*; Oct. 1990